Supplement of Atmos. Chem. Phys., 22, 11033–11047, 2022
https://doi.org/10.5194/acp-22-11033-2022-supplement

Atmospheric Chemistry and Physics Open Access

Supplement of

Measurement report: Observations of long-lived volatile organic compounds from the 2019–2020 Australian wildfires during the COALA campaign

Asher P. Mouat et al.

Correspondence to: Asher P. Mouat (amouat3@gatech.edu)

S1: PTR-ToF-MS and supporting observations

		Calibration Standards			
Compound	**Formula**	**m/z**	**Uncertainty (%)**	**In Standard**	**Limit of Detection (3σ, ppt)**
Methanol	CH_4OH^+	33.00	15	Yes	5
Acetonitrile	$C_2H_3NH^+$	42.03	15	Yes	5
Acetaldehyde	$C_2H_4OH^+$	45.03	15	Yes	5
Acrolein	$C_3H_4OH^+$	57.03	15	Yes	15
Acetone	$C_3H_6OH^+$	59.05	15	Yes	20
Isoprene	$C_5H_8H^+$	69.07	15	Yes	165
Methyl Vinyl Ketone	$C_4H_6OH^+$	71.05	15	Yes	5
Methacrolein	$C_4H_6OH^+$	71.05	15	Yes	5
Methyl Ethyl Ketone	$C_4H_8OH^+$	73.07	15	Yes	5
Benzene	$C_6H_6H^+$	79.05	15	Yes	10
Toluene	$C_7H_8H^+$	93.07	15	Yes	15
C_8-aromatics	$C_8H_{10}H^+$	107.09	15	Yes	5
Chlorobenzene	$C_5H_6ClH^+$	113.02	15	Yes	5
C_3-benzene	$C_9H_{12}H^+$	121.10	15	Yes	20
P-cymene	$C_{10}H_{14}H^+$	135.12	15	Yes	10
α-pinene	$C_{10}H_{16}H^+$	137.13	15	Yes	20
Cineole	$C_{10}H_{18}H^+$	155.14	15	Yes	20

Table S1: Standards used to calibrate PTR-TOF-MS as well as determine instrument transmission and limits of detection. Uncertainty of each compound is 15%.

Table S2: All reported EF species for this work and their respective uncertainties.

		All Presented Compounds		
Compound	**Formula**	**m/z**	**Uncertainty (%)**	**In Standard**
Methanol	CH_4OH^+	33.00	15	Yes
Acetonitrile	$C_2H_3NH^+$	42.03	15	Yes
Acetaldehyde	$C_2H_4OH^+$	45.03	15	Yes
Acrolein	$C_3H_4OH^+$	57.03	15	Yes
Acetone	$C_3H_6OH^+$	59.05	15	Yes
Isoprene	$C_5H_8H^+$	69.07	15	Yes
Methyl Vinyl Ketone	$C_4H_6OH^+$	71.05	15	Yes
Methacrolein	$C_4H_6OH^+$	71.05	15	Yes
Methyl Ethyl Ketone	$C_4H_8OH^+$	73.07	15	Yes
Benzene	$C_6H_6H^+$	79.05	15	Yes
m/z 85	$C_4H_4O_2H^+$	85.03	100	No
Methyl propanoate	$C_4H_8O_2H^+$	89.06	100	No
Toluene	$C_7H_8H^+$	93.07	15	Yes
Maleic Anhydride	$C_4H_2O_3H^+$	99.00	100	No
Methyl Methacrylate	$C_5H_8O_2H^+$	101.06	100	No
Benzaldehyde	$C_7H_6OH^+$	107.05	100	No
C_8-aromatics	$C_8H_{10}H^+$	107.09	15	Yes
Chlorobenzene	$C_5H_6ClH^+$	113.02	15	Yes
C_3-benzene	$C_9H_{12}H^+$	121.10	15	Yes
P-cymene	$C_{10}H_{14}H^+$	135.12	15	Yes
α-pinene	$C_{10}H_{16}H^+$	137.13	15	Yes
Cineole	$C_{10}H_{18}H^+$	155.14	15	Yes

S3: Plume Origin and Transport Time

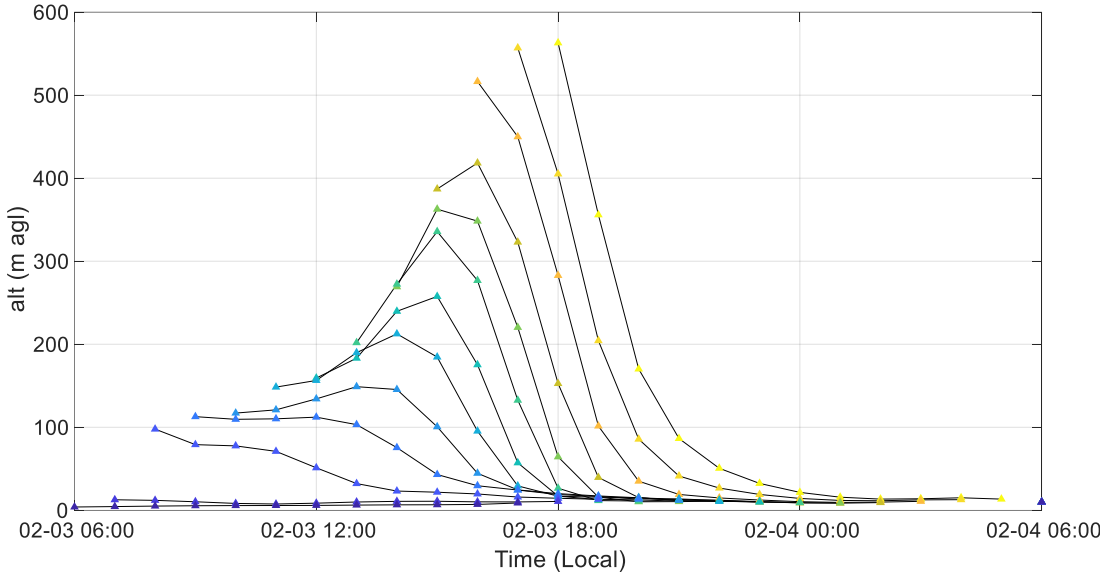

Figure S1: Altitudes corresponding by color to trajectories plotted in Fig. 1. For the periods closer to sunrise on 4 Feb 2020, the model predicts higher altitudes that reach 563 m agl at maximum. This resulted from air masses travelling over active fires. The decline in altitude results from these same masses travelling over the ocean which has less turbulent, cooler conditions.

There are two major clusters of fires emitting during the period over which we sampled smoke; the fires just to the south of Canberra (Fig. S3), and the two large clusters at the southeast (SE) corner (Figures S4 and S5) which mix into one plume. We examine both how these plumes interacted and the meteorological conditions surrounding the SE clusters. HYSPLIT forward trajectories are shown in Figures S3 and S4 using the same meteorological input and at the same altitude layers as in Fig. 1 from the main text.

In Fig. S3, the HYSPLIT forward trajectory shows that the plume from the Canberra fires was lofted to approximately 2000 m agl well before interacting with the SE-emitted plume, which ascended to 210 m agl as a maximum height (from Fig. S2, the upper limit is around 560 m agl). These trajectories indicate that little mixing would have occurred between these two plumes and that the plume from the SE is almost entirely what was sampled with only smaller fires along the eastern coast potentially contributing.

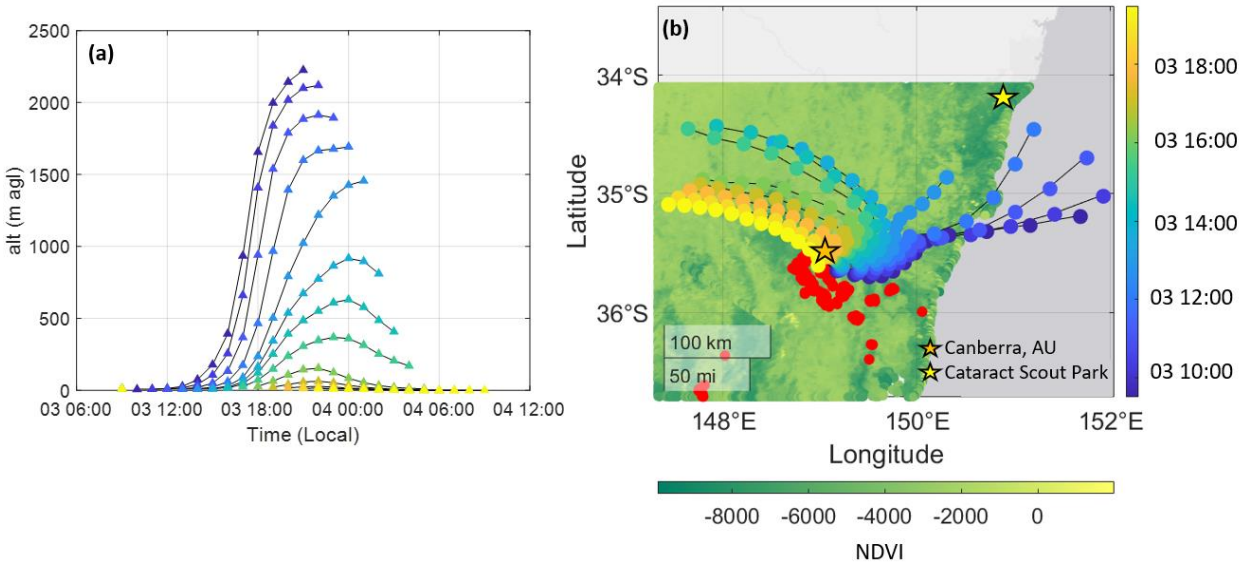

Figure S2: HYSPLIT forward trajectory starting at the centroid of the fire cluster to the south of Canberra, AU. This simulation was set to run at 10:30 on 3 Feb 2020 - 8 h in advance of when the PTR-ToF-MS began sampling smoke. Each tail moves forward in time 12 h, with a new tail plotted every hour. Panel (a) shows the altitude to which each trajectory was lofted, and panel (b) shows the spatial distribution of the plots as well as Canberra and Cataract Scout Park's location. Normalized difference vegetation index (NDVI) is also plotted to show greenery distribution, with darker green signifying denser foliage.

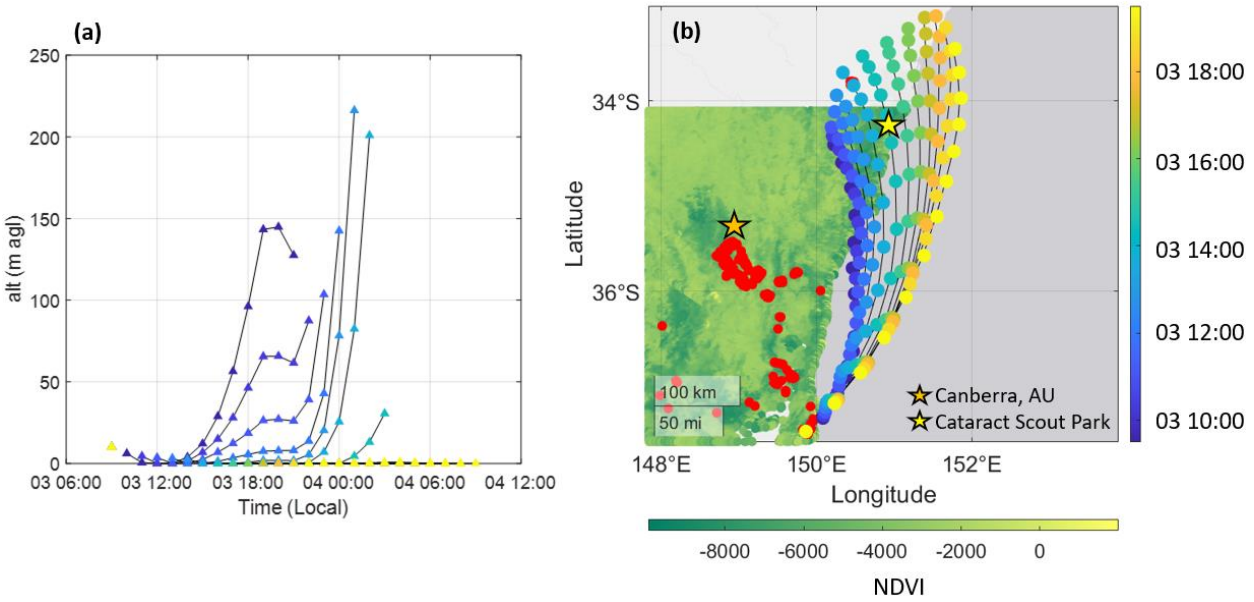

Figure S3: HYSPLIT forward trajectory starting at the southern fire cluster in the southeast corner of the country. This simulation was set to run at 10:30 on 3 Feb 2020 - 8 h in advance of when the PTR-ToF-MS began sampling smoke. Each tail moves forward in time 12 h, with a new tail plotted every hour. Panel (a) shows the altitude to which each trajectory was lofted, and panel (b) shows the spatial distribution of the plots as well as Canberra and Cataract Scout Park's location. Normalized difference vegetation index (NDVI) is also plotted to show greenery distribution, with darker green signifying denser foliage.

Figure S5 displays a closer view of the two active fires in the southeast (SE). These fires are spaced approximately 70 km apart and thus we check two major meteorological components to determine whether combustion conditions differed substantially – total precipitation and wind speed.

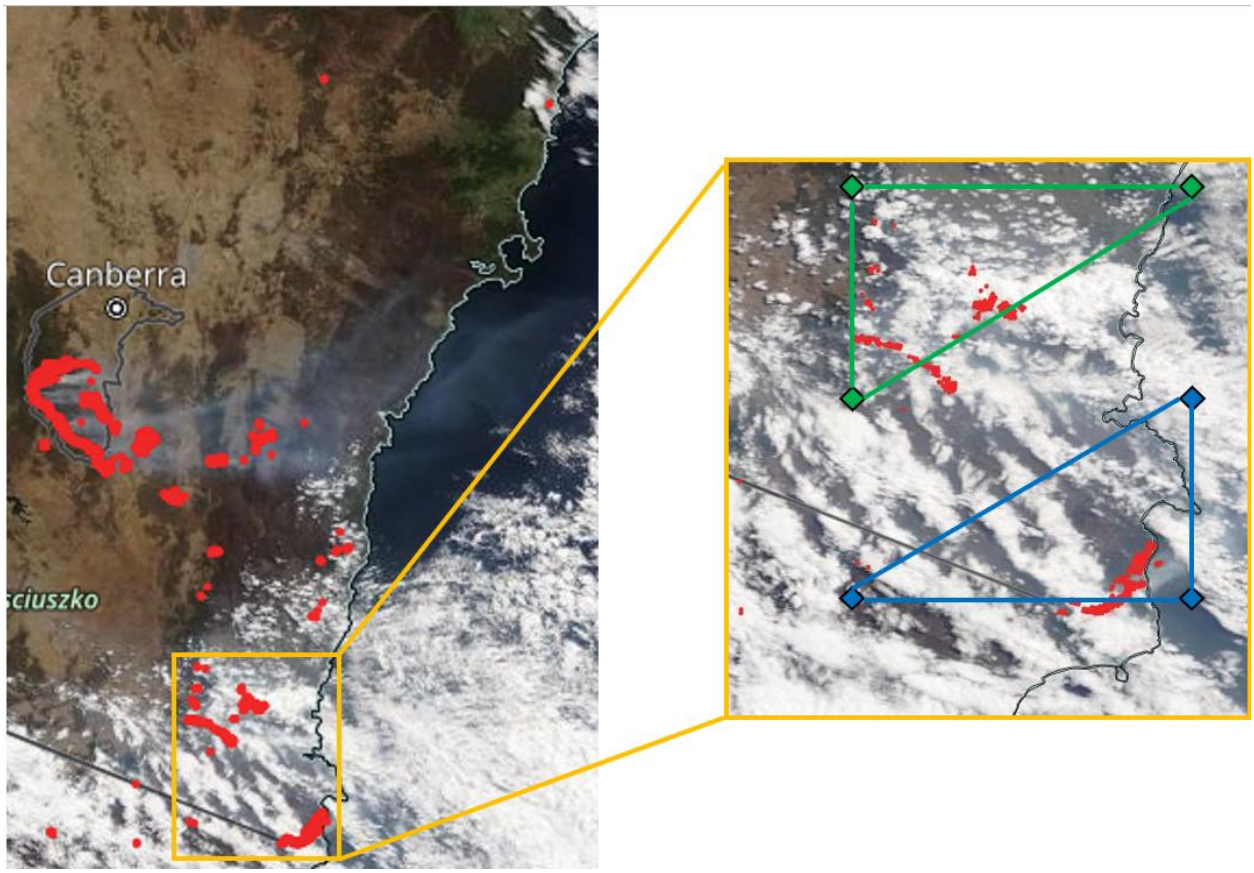

Figure S4: NASA Worldview imagery with fire counts plotted from the VNP14IMGTDL_NRT data from Suomi VIIRS satellite imaging. The left side of the graph shows the general location of the two southeast fire clusters which are termed the "north" (green triangle) and "south" (blue triangle) clusters. These active burning sites are approximately 70 km apart. The green and blue triangles on the right correspond to the indices over which average surface wind speed was calculated using data from MERRA-2.

Wind speed is calculated using hourly wind direction data from MERRA-2 measured at 10 m agl (Gelaro et al., 2017). This data has a spatial resolution of 0.5◦ x 0.625◦ and the corresponding coordinate points used for spatial averaging are shown on the right side of Fig. S5, with the green triangle overlaid on the northern fire cluster and the blue triangle on the southern. Results of hourly wind speed data are shown in Fig. S6 and indicate that despite the distance, both fires saw similar wind velocities before, during, and after the period the PTR-ToF-MS sampled smoke. This indicates that wind speed wouldn't have significantly affected combustion conditions.

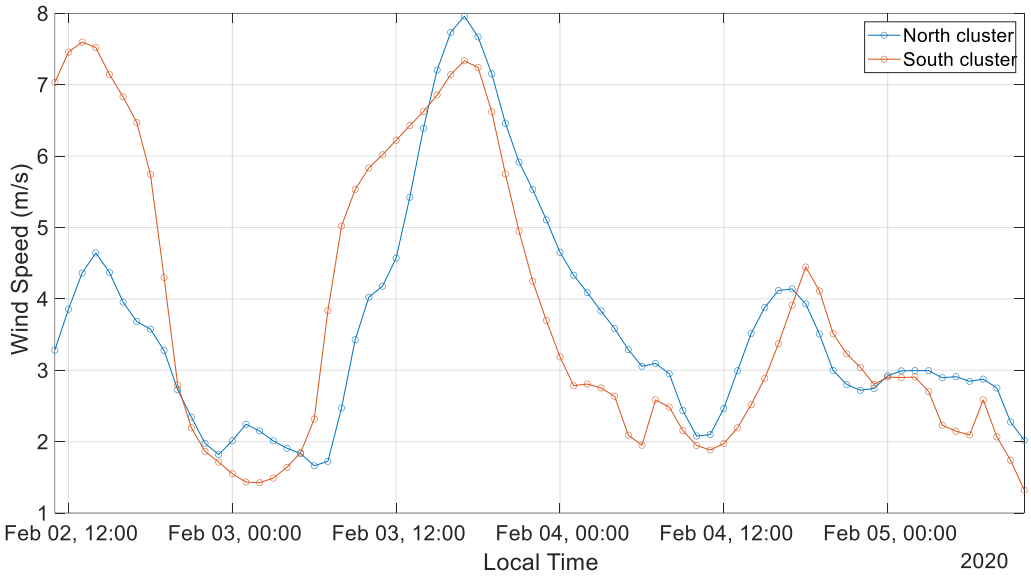

Figure S5: Hourly, spatially averaged wind speed for the northern and southern fire clusters corresponding to the green (northern) and blue (southern) triangles in Fig. S5. These values are calculated using hourly measurements of the U10M and V10M wind direction data from the MERRA-2 tavg1_2d_slv_Nx dataset at 0.5◦ x 0.625◦ resolution. Both clusters experience similar wind velocities before, during, and after the smoke event period over which the PTR-ToF-MS was sampling, further indicating similar combustion conditions for both fires.

Lastly, Fig. S7 shows modeled monthly average of total precipitation for the month of January 2020, preceding when the southeast fires started. This data is outputted from the Australian Bureau of Meteorology's Gridded Climate Data at a 0.05◦ x 0.05◦ resolution (Jones et al., 2009) with the image generated from the Australian Bureau of Meteorology's website. Both fire clusters in the southeast are active in similarly forested regions that experienced similar levels of precipitation, indicating that they should again be burning under similar combustion conditions. As such, we conclude that EFs derived from this plume are representative of a biome-averaged EF.

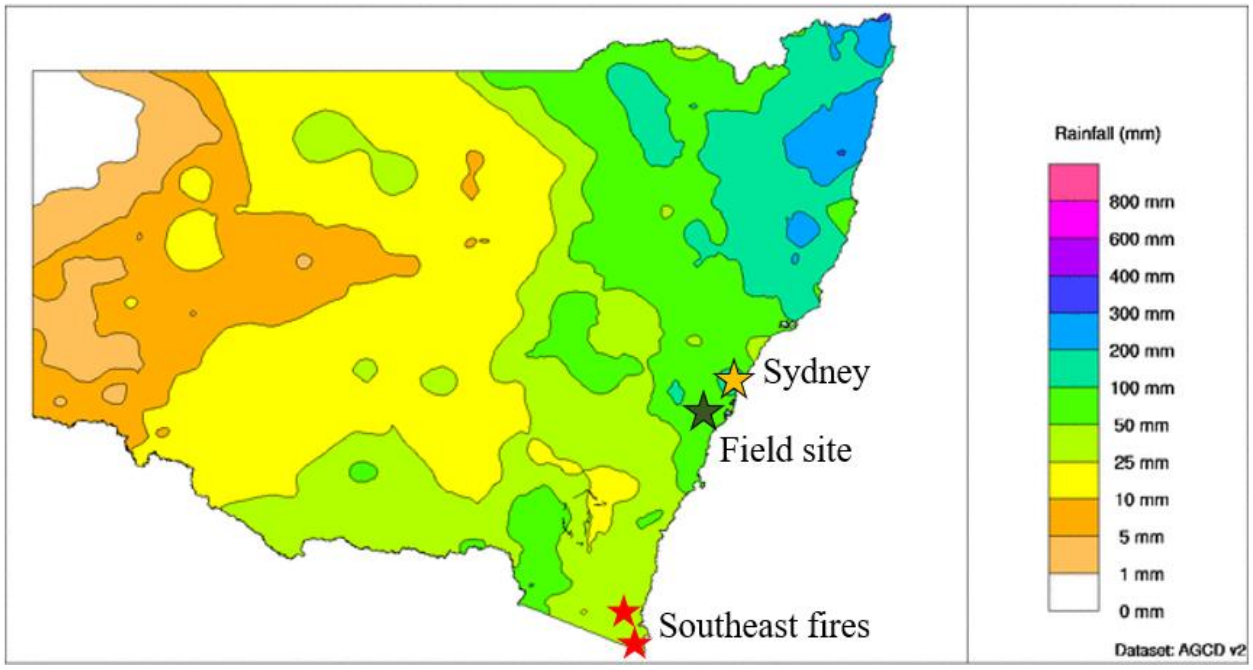

Figure S6: Daily total precipitation averaged over the month of January 2020 from the Australian Bureau of Meteorology's Gridded Climate Data at a resolution of 0.05◦ x 0.05◦., occurring prior to the southeast fires. Image generated from the Bureau of Meteorology website. Both clusters are in a region that has experienced similar total rainfall between 25-50mm.

S4: Calculating Emission Ratios

An emission ratio (ER) is the defined in this work as the slope of a linear regression of a VOC of interest (X) to CO (both in units of ppb). From methodology further discussed in Sect. 5.2 of the main paper, an $R^2 \geq 0.5$ is set to ensure a robust correlation. Fig. S2 shows a comparison between ERs derived from two subsets of data over the smoke event – one from the freshest portion of the plume and the other using an average from 4 subsets making up the entirety of the event.

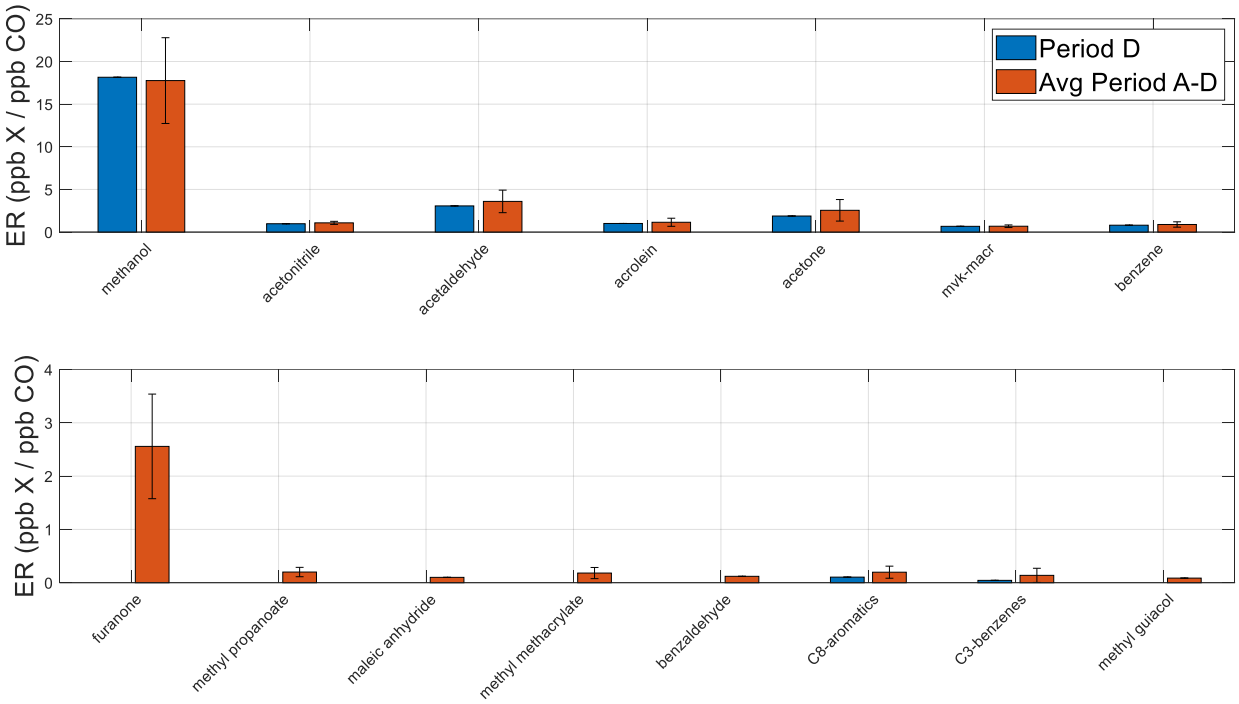

Figure S7: Comparison of ERs derived from solely period D and then from average of all periods. Standard deviation is reported for each average ER. If standard deviation is missing, then that compound had only one viable ER of the four periods. For all compounds here, variability is high enough to capture all period D ERs within 1σ.

Table S3: Emission ratios derived from averaging over periods A-D. Standard deviation is reported for each ER. Dashes indicated that only one of four periods had a viable ER.

Compound	Formula	m/z	Emission Ratios (ppt ppbCO^{-1})
Methanol	CH_4OH^+	33.00	17.97±5.08
Acetonitrile	$C_2H_3NH^+$	42.03	1.11±0.19
Acetaldehyde	$C_2H_4OH^+$	45.03	3.67±1.30
Acrolein	$C_3H_4OH^+$	57.03	1.19±0.42
Acetone	$C_3H_6OH^+$	59.05	2.70±1.36
MVK+MACR	$C_4H_6OH^+$	71.05	0.71±0.13
Benzene	$C_6H_6H^+$	79.05	0.93±0.28
m/z 85	$C_4H_4O_2H^+$	85.03	2.84±0.91
Methyl propanoate	$C_4H_8O_2H^+$	89.06	0.21±0.10
Maleic anhydride	$C_4H_2O_3H^+$	99.00	0.14±--
Methyl methacrylate	$C_5H_8O_2H^+$	101.06	0.19±0.12
Benzaldehyde	$C_7H_6OH^+$	107.05	0.14±--
C_8-aromatics	$C_8H_{10}H^+$	107.09	0.22±0.13
C_3-benzene	$C_9H_{12}H^+$	121.10	0.17±0.15
Creosol	$C_8H_{10}O_2H^+$	139.08	0.10±--

S5: Emission Factors

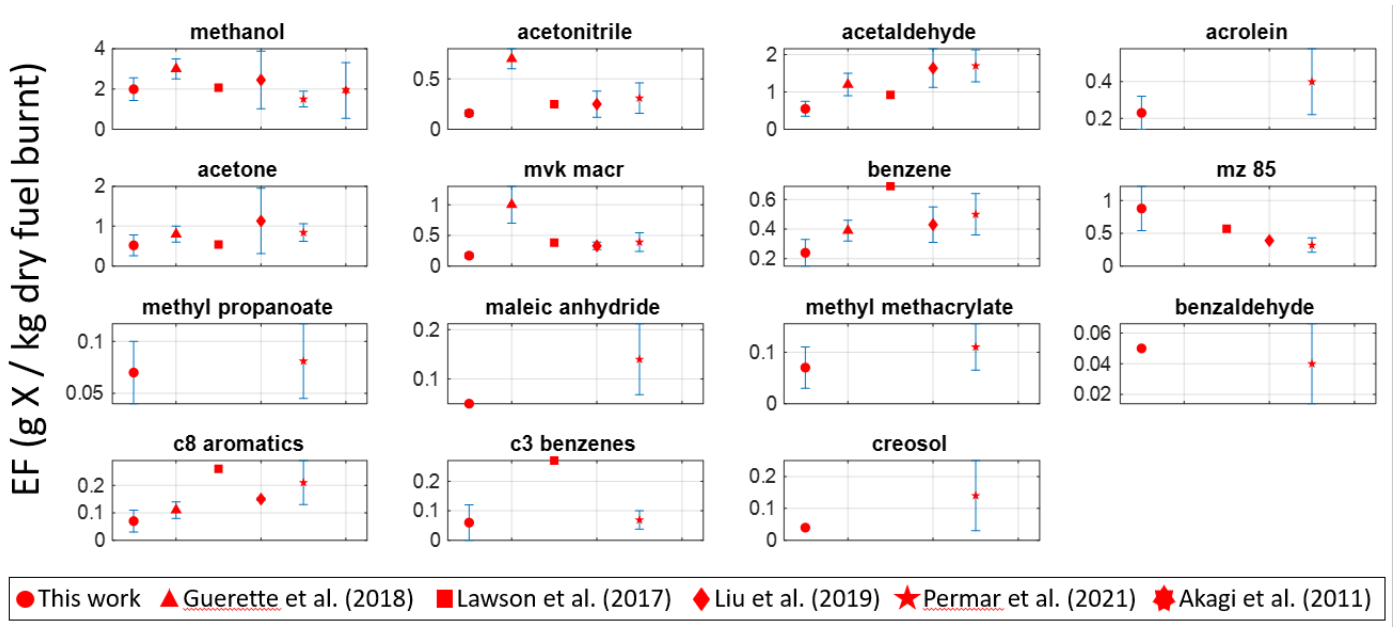

Figure S8: Scatter plot version of all reported emission factors and uncertainty plotted for all studies that this work was compared to.

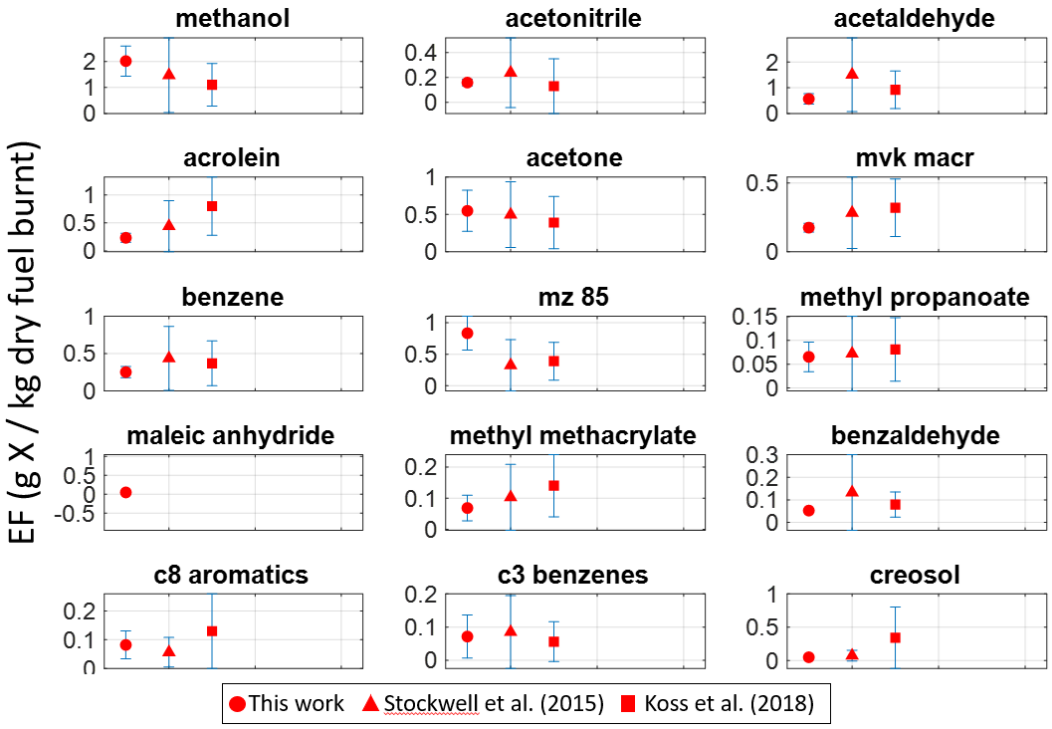

Figure S9: Scatter plots showing EFs calculated in this work alongside those calculated from laboratory based, individual fuel type studies wherein the fuels are all located in temperate U.S. forests. Values from Koss et al. (2018) are the EF averages over all fuel types. Values from Stockwell et al. (2015) are determined from selecting a subgroup of fuel types present in temperate forests (e.g. excluding cooking emissions of fuel types from savannahs).

EFs calculated from this work show excellent agreement with values from both Stockwell et al. (2015) and Koss et al. (2018) with virtually every compound within uncertainty. These results indicate the ability to even employ lab-based, averaged EFs across geographically separate but analogous biomes.

References:

Gelaro, R., McCarty, W., Suárez, M. J., Todling, R., Molod, A., Takacs, L., Randles, C. A., Darmenov, A., Bosilovich, M. G., Reichle, R., Wargan, K., Coy, L., Cullather, R., Draper, C., Akella, S., Buchard, V., Conaty, A., da Silva, A. M., Gu, W., Kim, G.-K., Koster, R., Lucchesi, R., Merkova, D., Nielsen, J. E., Partyka, G., Pawson, S., Putman, W., Rienecker, M., Schubert, S. D., Sienkiewicz, M., and Zhao, B.: The Modern-Era Retrospective Analysis for Research and Applications, Version 2 (MERRA-2), Journal of Climate, 30, 5419-5454, 10.1175/jcli-d-16-0758.1, 2017.

Jones, D. A., Wang, W., and Fawcett, R.: High-quality spatial climate data-sets for Australia, Australian Meteorological and Oceanographic Journal, 58, 233, 2009.

Koss, A. R., Sekimoto, K., Gilman, J. B., Selimovic, V., Coggon, M. M., Zarzana, K. J., Yuan, B., Lerner, B. M., Brown, S. S., Jimenez, J. L., Krechmer, J., Roberts, J. M., Warneke, C., Yokelson, R. J., and de Gouw, J.: Non-methane organic gas emissions from biomass burning: identification, quantification, and emission factors from PTR-ToF during the FIREX 2016 laboratory experiment, Atmos. Chem. Phys., 18, 3299-3319, 10.5194/acp-18-3299-2018, 2018.

Stockwell, C. E., Veres, P. R., Williams, J., and Yokelson, R. J.: Characterization of biomass burning emissions from cooking fires, peat, crop residue, and other fuels with high-resolution proton-transfer-reaction time-of-flight mass spectrometry, Atmos. Chem. Phys., 15, 845-865, 10.5194/acp-15-845-2015, 2015.